

Single-Phase Full-Wave Rectifier as an Effective Example to Teach Normalization, Conduction Modes, and Circuit Analysis Methods

Predrag Pejović, Johann W. Kolar

Abstract—Application of a single phase rectifier as an example in teaching circuit modeling, normalization, operating modes of nonlinear circuits, and circuit analysis methods is proposed. The rectifier supplied from a voltage source by an inductive impedance is analyzed in the discontinuous as well as in the continuous conduction mode. Completely analytical solution for the continuous conduction mode is derived. Appropriate numerical methods are proposed to obtain the circuit waveforms in both of the operating modes, and to compute the performance parameters. Source code of the program that performs such computation is provided.

Index Terms—Circuit analysis, circuit modeling, computer aided analysis, electrical engineering education, power engineering education, rectifiers.

Original Research Paper

DOI: 10.7251/ELS1317123P

I. INTRODUCTION

Application of numerical computation tools in teaching practice is in increase, following increased application of numerical tools in engineering practice. This includes both application of specialized electronic circuit simulation tools [1], [2], and general purpose numerical computation tools [3]. However, wide application of simulation software did not replace the analytical approach completely, since the analytical approach provides deeper insight into circuit operation and provides better understanding, which is of interest for design engineers.

Analysis of single-phase rectifiers is inevitable part of every general electronics course [4, pp. 179–190], or power electronics course [5, pp. 82–100]. These circuits contain low number of elements, but expose rather complex behavior in the case some sort of filtering is applied. This makes the single-phase rectifiers an excellent example to teach some fundamental methods in nonlinear circuit analysis. A numerical approach to this problem could be found in [3, pp. 231–235]. On the other hand, analytical approach in teaching single-phase full-wave rectifiers with capacitive filtering is discussed in detail in [6] and [7]. These analyses are focused to the rectifiers supplied from an ideal voltage source. However, impedance

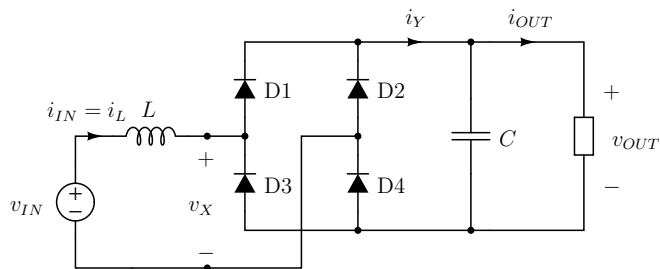


Fig. 1. The rectifier.

of the supplying source might be significant in practice [5, page 82], especially if the rectifier is supplied by a small transformer.

In this paper, analysis of the circuit shown in Fig. 1 is presented from an educational point of view. It is assumed that the supplying source might be represented as a series connection of an ideal voltage source and the source inductance L . The filtering capacitor is assumed to be large enough to neglect the output voltage ripple. This circuit is proposed as a nice example to teach circuit modeling, normalization, operating modes, conduction angle, and circuit analysis techniques. The approach has been successfully tested in teaching practice [8]. An approach to analyze this circuit is also presented in [5, pp. 91–95].

II. PRELIMINARY ANALYSIS, NORMALIZATION, AND ANALYSIS OF THE DISCONTINUOUS CONDUCTION MODE

Let us assume that the rectifier of Fig. 1 is supplied by the voltage source

$$v_{IN} = V_m \sin(\omega t). \quad (1)$$

To simplify the analysis, let us also assume that the capacitance of the filter capacitor is large enough to justify the approximation that the output voltage is constant in time. At this time point, we are going to continue the rectifier analysis as if the rectifier output voltage V_{OUT} is known. Thus, the output part of the rectifier, consisting of the filtering capacitor and the load could be replaced by a constant voltage source of the voltage V_{OUT} , as depicted in Fig. 2, which would not cause any change in the remaining part of the circuit. The diode bridge operates such that for $i_L > 0$ diodes D1 and D3 are conducting, resulting in $i_Y = i_L$ and $v_X = V_{OUT}$. On the other hand, for $i_L < 0$ diodes D2 and D4 are conducting,

Manuscript received 1 December 2013. Received in revised form 25 December 2013. Accepted for publication 26 December 2013.

P. Pejović is with the University of Belgrade, School of Electrical Engineering, 11120 Belgrade, Serbia (e-mail: peja@etf.rs).

J. W. Kolar is with the Power Electronic Systems Laboratory, Swiss Federal Institute of Technology Zurich, ETH-Zentrum/ETL, CH-8092 Zurich, Switzerland (e-mail: kolar@lem.ee.ethz.ch).

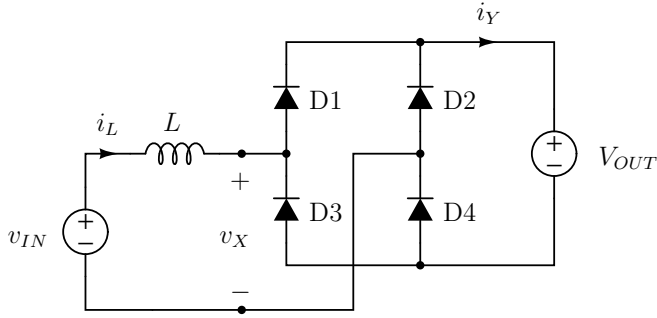


Fig. 2. Rectifier model applied in the analysis.

resulting in $i_Y = -i_L$ and $v_X = -V_{OUT}$. However, these two situations do not exhaust all of the conduction possibilities. In the case $i_L = 0$, input port of the diode bridge can stand any voltage in the range $-V_{OUT} < v_X < V_{OUT}$. An additional constraint that $di_L/dt = 0$ causes $v_X = v_{IN}$. The additional constraint requires that the inductor current is equal to zero over an interval of time. Thus, the result for the diode bridge input voltage v_X for $i_L = 0$ is obtained analyzing the remaining part of the circuit, not the diode bridge itself. In the case the inductor is replaced by a resistor, the additional constraint regarding the current derivative over time would not be necessary, but the result for v_X would be the same.

Thus, equations that characterize the diode bridge loaded with a voltage source could be summarized by the diode bridge input voltage equation

$$v_X = \begin{cases} V_{OUT}, & \text{for } i_L > 0 \\ v_{IN}, & \text{for } i_L = 0 \text{ and } \frac{di_L}{dt} = 0 \\ -V_{OUT}, & \text{for } i_L < 0 \end{cases} \quad (2)$$

and the diode bridge output current equation

$$i_Y = |i_L|. \quad (3)$$

It is worth to mention here that product $v_X i_L$ always provides a nonnegative value. Thus, the diode bridge rectifier behaves like a power sink, and there is no power that could be recovered from the diode bridge input terminals.

Assuming ideal filtering, the rectifier output current would contain only a DC component I_{OUT} equal to the average value of i_Y , while the AC component of i_Y would be taken by the filtering capacitor. In this manner, the rectifier output current for an assumed output voltage will be computed as the average value of i_Y .

Let us start the rectifier analysis from high output voltages, for $V_{OUT} > V_m$. In this case, the diodes in the diode bridge would be reverse biased during the whole period, resulting in $i_L = 0$, $i_Y = 0$, and $I_{OUT} = 0$. Thus, this situation to happen in practice would require an additional source to be connected at the rectifier output.

Lowering the output voltage slightly below V_m would cause the diodes D1 and D3 to start conducting at

$$V_m \sin(\alpha) = V_{OUT} \quad (4)$$

as illustrated in the first diagram of Fig. 3. It can be concluded that the conduction start angle α depends on two variables,

the output voltage and the input voltage amplitude. Actually, the conduction start angle depends on the ratio of these two variables. Thus, to generalize the analysis it is convenient to introduce a normalization of the rectifier voltages and to replace all the voltages with their normalized equivalents according to

$$m_Z = \frac{v_Z}{V_m} \quad (5)$$

i.e. taking the amplitude of the input voltage as the normalization basis. In this manner, the conduction start angle is obtained from

$$\sin(\alpha) = \frac{V_{OUT}}{V_m} = M_{OUT}. \quad (6)$$

Equation that governs the inductor current in this half-cycle is

$$L \frac{di_L}{dt} = V_m (\sin(\omega t) - M_{OUT}) \quad (7)$$

which can be transformed to

$$\frac{\omega L}{V_m} \frac{di_L}{d(\omega t)} = \sin(\omega t) - M_{OUT}. \quad (8)$$

To simplify the notation further, normalization of currents naturally arises as

$$j_X = \frac{\omega L}{V_m} i_X \quad (9)$$

followed by the normalization of time

$$\varphi = \omega t \quad (10)$$

which effectively replaces the time variable with the phase angle variable. In this manner, the inductor equation in this half-period is simplified to

$$\frac{dj_L}{d\varphi} = \sin(\varphi) - M_{OUT} \quad (11)$$

having the solution

$$j_L(\varphi) = j_L(\alpha) + \int_{\alpha}^{\varphi} (\sin(\theta) - M_{OUT}) d\theta. \quad (12)$$

Since $j_L(\alpha) = 0$, the inductor current is given by

$$j_L(\varphi) = \cos(\alpha) + M_{OUT} \alpha - \cos(\varphi) - M_{OUT} \varphi \quad (13)$$

which is plotted in the second and the fifth of the diagrams of Fig. 3, and remains positive while $\varphi < \beta$, where $j_L(\beta) = 0$, i.e.

$$\cos(\alpha) + M_{OUT} \alpha - \cos(\beta) - M_{OUT} \beta = 0. \quad (14)$$

This situation could also be explained graphically, applying volt-second balance on the inductor voltage waveform, as depicted in the first diagram of Fig. 3. According to that explanation, the inductor current flows until the integral of the inductor voltage over time is different than zero. When the integral reaches zero, the inductor current reaches the initial current, zero in this situation. In the case

$$-m_{IN}(\beta) < M_{OUT} \quad (15)$$

all of the diodes in the diode bridge would remain reverse biased over the phase angle interval $\beta < \varphi < \alpha + \pi$, when diodes D2 and D4 would start to conduct since

$$-m_{IN}(\alpha + \pi) = M_{OUT} \quad (16)$$

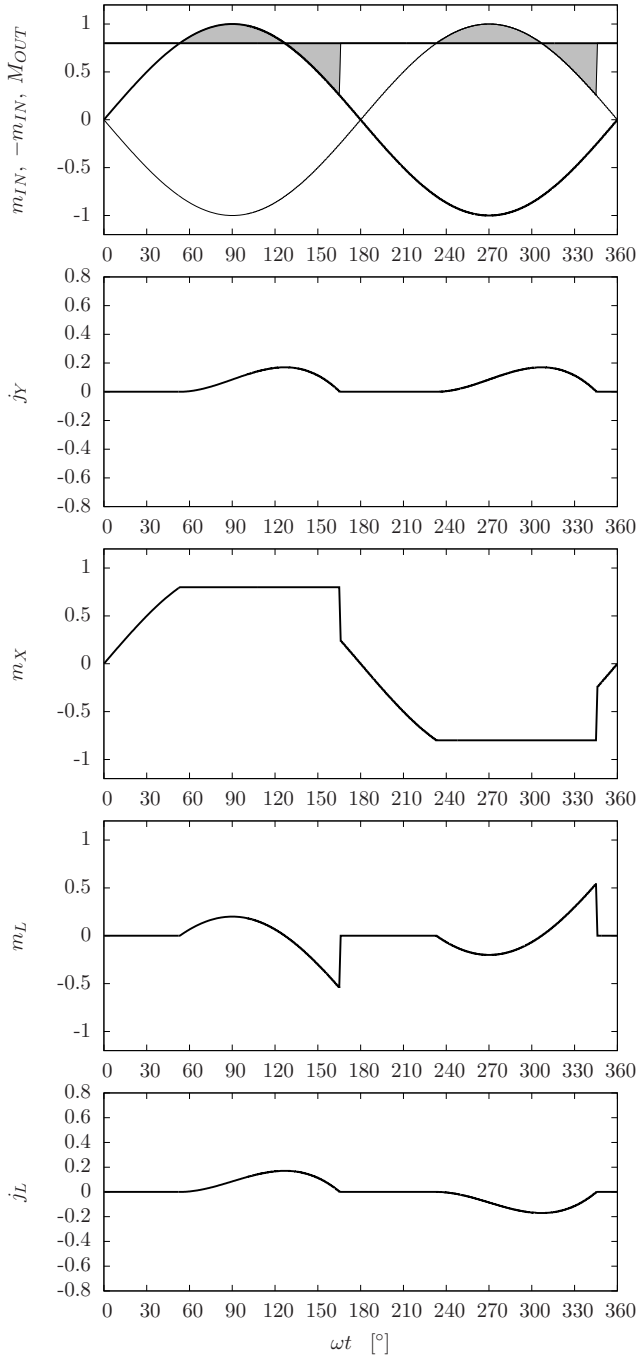


Fig. 3. Waveforms of the rectifier voltages and currents in the discontinuous conduction mode for $M_{OUT} = 0.8$.

as depicted in the first diagram of Fig. 3.

Operating mode when the inductor current stops and remains zero over a time interval is referred to as the discontinuous conduction mode. Thus, diagrams of Fig. 3 represent waveforms of the rectifier voltages and currents in the discontinuous conduction mode. Time intervals when j_L and j_Y are equal to zero could be observed. Conducting diodes are labeled on the waveform of m_X .

Equation (14) that determines phase angle β when the inductor current flow stops does not have a closed form solution. This is the limiting factor for obtaining an analytical

solution for the discontinuous conduction mode. Thus, the solution should be obtained numerically.

Analysis of the rectifier performed this far covers only one half-period of the rectifier operation, for $\alpha < \varphi < \alpha + \pi$. Applying symmetry, both of the circuit and the input voltage, we may conclude that in steady state

$$j_L(\varphi) = -j_L(\varphi + \pi). \quad (17)$$

The same conclusion applies for all variables at the AC side of the rectifier, including m_L and m_X , as it can be observed from the last three diagrams of Fig. 3.

Phase angle interval when $j_L < 0$ is named the conduction angle, and it is determined by

$$\gamma = \beta - \alpha. \quad (18)$$

In the case the rectifier operates in the discontinuous conduction mode, $\gamma < \pi$. For $\gamma = \pi$, the converter switches to the continuous conduction mode, which would result in entirely different behavior of the rectifier.

III. ANALYSIS OF THE RECTIFIER IN THE CONTINUOUS CONDUCTION MODE

In the case

$$-m_{IN}(\beta) > M_{OUT} \quad (19)$$

the inductor current continues to decrease after it reached zero, taking negative values. This situation corresponds to the rectifier operating in the continuous conduction mode. Applying symmetry arguments, we may conclude that $\gamma = \pi$ in this case. Extending the definition of α to the phase angle when the inductor current starts to grow from zero, we have

$$j_L(\alpha + \pi) = j_L(\alpha) = 0 \quad (20)$$

and even more important, equation (13) for the inductor current applies over the whole half-period $\alpha < \varphi < \alpha + \pi$. Applying (13) in (20), in the continuous conduction mode we have

$$\cos(\alpha) + M_{OUT} \alpha - \cos(\alpha + \pi) - M_{OUT}(\alpha + \pi) = 0 \quad (21)$$

which reduces to

$$\cos(\alpha) = \frac{\pi}{2} M_{OUT}. \quad (22)$$

This is one of the differences between the conduction modes, in the discontinuous conduction mode the inductor current starts to grow from zero at the phase angle determined by (6), while in the continuous conduction mode this angle is determined by (22). At the boundary between the modes both of the equations for α apply, resulting in the conduction starting angle α at the boundary between the modes

$$\tan(\alpha_{MC}) = \frac{2}{\pi} \quad (23)$$

and the corresponding normalized output voltage

$$M_{OUT MC} = \frac{2}{\sqrt{4 + \pi^2}} \approx 0.5370. \quad (24)$$

After the conduction starting angle is determined by (22), the inductor current is from (13) obtained as

$$j_L(\varphi) = M_{OUT} \left(\frac{\pi}{2} + \arccos\left(\frac{\pi}{2} M_{OUT}\right) - \cos(\varphi) - M_{OUT} \varphi \right) \quad (25)$$

during the half-period $\alpha < \varphi < \alpha + \pi$. During the other half-period, the input current waveform could be computed applying (17).

Waveforms of the voltages and currents for the rectifier operating in the continuous conduction mode at $M_{OUT} = 0.5$ are presented in Fig. 4. The diagrams are plotted applying the same scale as applied in the diagrams of Fig. 3, to illustrate increased magnitudes of currents in the continuous conduction mode. In the first diagram of Fig. 4, it should be noticed that condition (19) applies. Volt-second balance over the half-period is highlighted in the same diagram.

The rectifier output current is obtained as the average of the diode bridge output current j_Y , which in terms of j_L reduces to

$$J_{OUT} = \frac{1}{\pi} \int_{\alpha}^{\alpha+\pi} j_L(\varphi) d\varphi = \frac{2}{\pi} \sin(\alpha). \quad (26)$$

Such integral is harder to compute for the discontinuous conduction mode, due to the difficulties in obtaining the upper limit of integration, β .

Substituting the value of α obtained from (22), dependence of the output current on the output voltage in the continuous conduction mode is obtained as

$$J_{OUT} = \frac{1}{\pi} \sqrt{4 - \pi^2 M_{OUT}^2} \quad (27)$$

meaning that the rectifier output characteristic in the normalized output plane (J_{OUT}, M_{OUT}) is a circle with the radius equal to $2/\pi$, $M_{OUT}^2 + J_{OUT}^2 = (2/\pi)^2$. Applying the rectifier output characteristic (27), the rectifier short circuit current is obtained as

$$J_{OUT SC} = \frac{2}{\pi} \approx 0.6366 \quad (28)$$

while the output current when the rectifier changes its operating mode is

$$J_{OUT SC} = \frac{4}{\pi \sqrt{4 + \pi^2}} \approx 0.3419. \quad (29)$$

The RMS value of the rectifier input current is analytically obtained as

$$J_{IN RMS} = \frac{\sqrt{3}}{6} \sqrt{6 + (\pi^2 - 24) M_{OUT}^2} \quad (30)$$

which is an important parameter to design the input transformer.

Normalized value of the rectifier output power is

$$P_{OUT} = M_{OUT} J_{OUT} = \frac{M_{OUT}}{\pi} \sqrt{4 - \pi^2 M_{OUT}^2} \quad (31)$$

and this curve exposes maximum at

$$M_{OUT P MAX} = \frac{\sqrt{2}}{\pi} \quad (32)$$

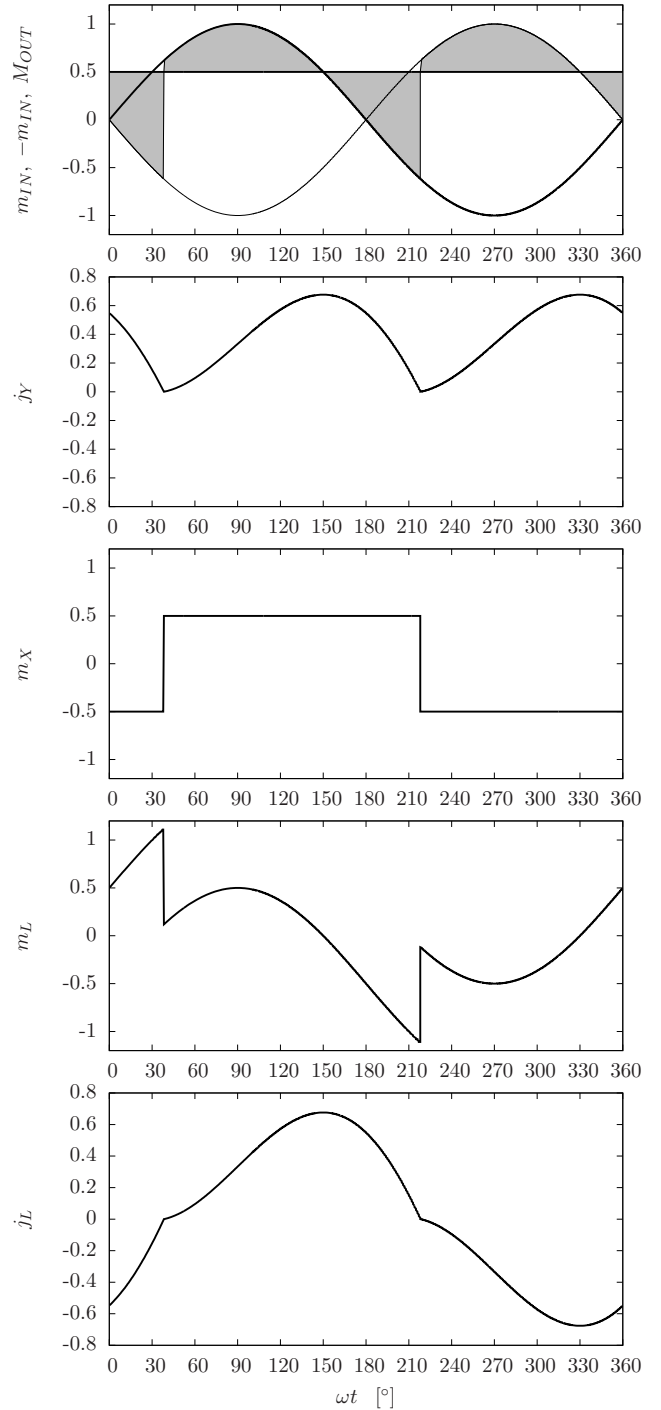


Fig. 4. Waveforms of the rectifier voltages and currents in the continuous conduction mode for $M_{OUT} = 0.5$.

which is within the continuous conduction operating range. The maximum of the DC power that the rectifier could supply to the load is

$$P_{OUT MAX} = \frac{2}{\pi^2} \text{ p.u.} \approx 0.2026 \text{ p.u.} \quad (33)$$

Since the commutation angles α and β are available in closed form for the continuous conduction mode, many analytical results for the parameters that characterize the rectifier operation are available in closed form. To obtain values of

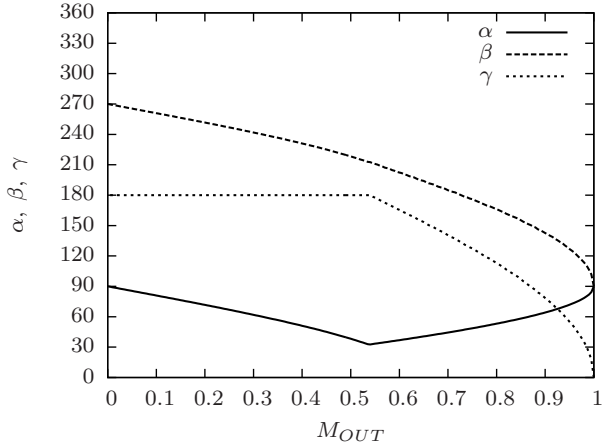
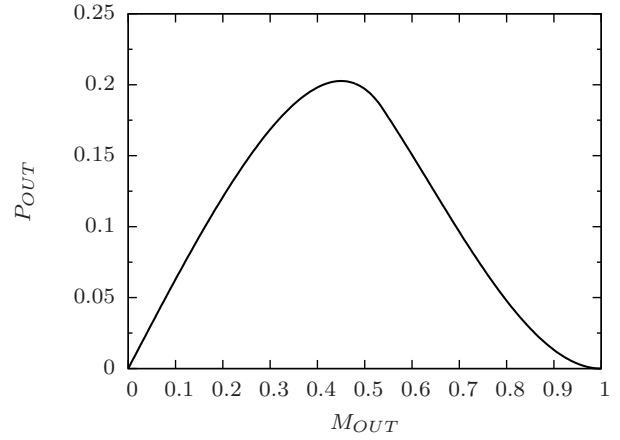
Fig. 5. Dependence of α , β , and γ on M_{OUT} .

Fig. 7. Dependence of the rectifier output power on the output voltage.

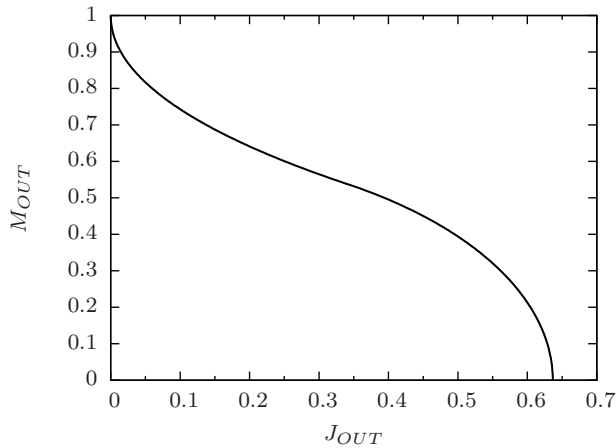


Fig. 6. Dependence of the rectifier output voltage on the output current.

these parameters for the rectifier operating in the discontinuous conduction mode, numerical methods should be applied.

IV. NUMERICAL SIMULATION OF THE RECTIFIER OPERATION

After the analysis of the rectifier is performed, numerical implementation of the model is a straightforward procedure. A GNU Octave program that “plays a cartoon” illustrating the rectifier operation for the whole range of the output voltage values is given in the Appendix. Source code is available at <http://tnt.etf.bg.ac.rs/~oe3ee/singlephase.m>, while Python version of the same program (PyLab) is available at <http://tnt.etf.bg.ac.rs/~oe3ee/singlephase.py>. Some of the diagrams that the program provides as a result are presented here.

In Fig. 5, dependence of the phase angle when the inductor current becomes positive, α , the phase angle when the inductor current falls to zero, β , and the conduction angle γ on M_{OUT} are presented. Transition between the modes could clearly be observed in the diagrams $\alpha(M_{OUT})$ and $\gamma(M_{OUT})$.

Dependence of the rectifier output voltage on the output current is presented in Fig. 6. The diagram of Fig. 6 is obtained

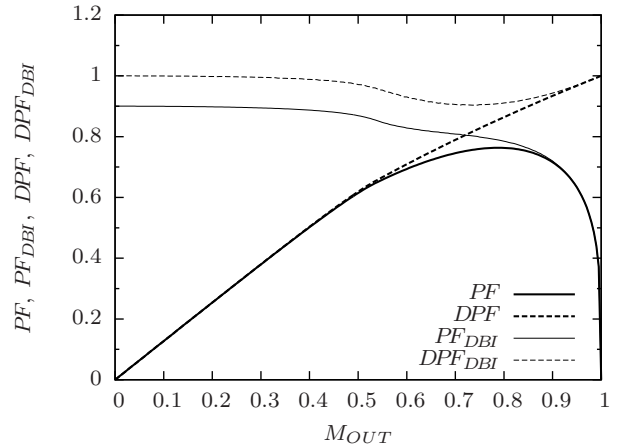


Fig. 8. Dependence of power factors and displacement power factors on the output voltage.

by numerical computation, but in the continuous conduction mode matches the analytical result (27). Dependence of the output power on the output voltage is presented in Fig. 7. The curve is obtained applying numerical computation, but in the continuous conduction mode matches the analytical result (31) and reaches maximum according to (32) and (33).

Other parameters, like the total harmonic distortions of the input current and the voltage at the rectifier input, as well as the RMS value of the input current, may be computed. As an illustration, values of the power factor and the displacement power factor at the ideal voltage source, PF and DPF , as well as at the diode bridge input terminals, PF_{DBI} and DPF_{DBI} are presented in Fig. 8. This diagram may be applied as an illustration while introducing definitions of power factor and the displacement power factor, since differences between these two parameters are clearly observable on an example encountered in practice.

V. CONCLUSIONS

In this paper, a single-phase full-bridge rectifier supplied by a source with finite leakage inductance is proposed as an effective example to teach circuit modeling, normalization, operating modes, and various techniques of circuit analysis. Discontinuous conduction mode is analyzed, and it is shown why an analytical closed form solution cannot be obtained. On the other hand, an analytical solution is derived for the continuous conduction mode. During the circuit analysis, appropriate normalization is introduced to generalize the results. A numerical method to compute the rectifier waveforms in both of the operating modes is presented, and a GNU Octave program that illustrates the circuit behavior and may be used for educational purposes is provided. Diagrams of various parameters that characterize the rectifier operation, provided by numerical computation, are presented. The circuit analyzed in the paper is simple and reach in phenomena of educational interest that it might be used as a laboratory example, as well.

VI. APPENDIX

```

np = 180 * 2; # could be adjusted if the simulation is too slow
step = 0.005; # could be adjusted if there are too many points

np2 = 2 * np;

i = 1 : np2;
wt = 2 * pi / np2 * (i - 0.5);
deg = wt * 180 / pi;

minp = sin(wt);
co = cos(wt);

Mboundary = 2 / sqrt(4 + pi^2);

counter = 0;
for Mout = 1 - step : -step : step
    counter = counter + 1;
    mout(counter) = Mout;
    if Mout > Mboundary
        dcm(counter) = 1;
        colour = 'b';
        alpha = asin(Mout);
        a(counter) = alpha * 180 / pi;
        nalpha = find(wt > alpha, 1) - 1;
        j10 = cos(alpha) + Mout * alpha;
        for i = 1 : np
            j(i) = j10 - co(nalpha + i) - Mout * wt(nalpha + i);
        end
        nbeta = find(j < 0, 1);
        b(counter) = nbeta / np * 180 + a(counter);
        j(nbeta : np) = zeros(1, np - nbeta + 1);
    else
        dcm(counter) = 0;
        colour = 'r';
        alpha = acos(pi / 2 * Mout);
        a(counter) = alpha * 180 / pi;
        b(counter) = a(counter) + 180;
        nalpha = find(wt > alpha, 1) - 1;
        j10 = cos(alpha) + Mout * alpha;
        for i = 1 : np
            j(i) = j10 - co(nalpha + i) - Mout * wt(nalpha + i);
        end
    end
    j1(1 : np) = j;
    j1(np + 1 : np2) = -j;
    j1 = circshift(j1', nalpha');
    mx = minp .* (j1 == 0) + Mout * ((j1 > 0) - (j1 < 0));
    ml = minp - mx;
    jy = abs(j1);
    jout(counter) = mean(jy);
    pout(counter) = Mout * jout(counter);

figure(1)

subplot(2, 2, 1)
plot(deg, j1, colour)
axis([0 360 -1.1 1.1])
set(gca, 'xtick', 0 : 360 : 30)
xlabel('wt [deg]')
ylabel('j1')

subplot(2, 2, 3)
plot(deg, ml, colour)
axis([0 360 -1.5 1.5])
set(gca, 'xtick', 0:360:30)
xlabel('wt [deg]')
ylabel('ml')

subplot(2, 2, 4)
plot(deg, mx, colour)
axis([0 360 -1.5 1.5])

```

```

set(gca, 'xtick', 0 : 360 : 30)

subplot(2, 2, 2)
plot(deg, jy, colour)
xlabel('wt [deg]')
ylabel('jy')
axis([0 360 -1.1 1.1])
set(gca, 'xtick', 0 : 360 : 30)

pause(0.5)

xin = measure(j1, minp);
pin(counter) = xin(1);
pf(counter) = xin(3);
dpf(counter) = xin(4);
thdi(counter) = xin(5);
jrms(counter) = xin(8);
xpcc = measure(j1, mx);
pinpcc(counter) = xpcc(1);
pfpcc(counter) = xpcc(3);
dpfpcc(counter) = xpcc(4);
thdv(counter) = xpcc(6);

end

figure(2)
plot(mout, jout)
xlabel('Mout')
ylabel('Jout')

figure(3)
plot(jout, mout)
xlabel('Jout')
ylabel('Mout')

figure(4)
plot(mout, pin, 'r', mout, pinpcc, 'g', mout, pout, 'b')
xlabel('Mout')
ylabel('Pin, Pinpcc, Pout')

figure(5)
plot(mout, pf, 'b', mout, pfpcc, 'r')
xlabel('Mout')
ylabel('PF [blue], PFPcc [red]')

figure(6)
plot(mout, dpf, 'b', mout, dpfpcc, 'r')
xlabel('Mout')
ylabel('DPF [blue], DFPpcc [red]')

figure(7)
plot(mout, thdi)
xlabel('Mout')
ylabel('THDi')

figure(8)
plot(mout, thdv)
xlabel('Mout')
ylabel('THDv')

figure(9)
plot(mout, a, 'b', mout, b, 'g', mout, b - a, 'r')
xlabel('Mout')
ylabel('alpha [blue], beta [green], gama [red]')

function x = measure(i, v)

    n = size(i, 2);
    I = fft(i);
    V = fft(v);

    irms = sqrt(mean(i .* i));
    vrms = sqrt(mean(v .* v));

    ilrms = sqrt(2) * abs(I(2)) / n;
    vlrms = sqrt(2) * abs(V(2)) / n;

    p = mean(i .* v);

    s = irms * vrms;

    pf = p / s;

    dpf = cos(angle(I(2)) - angle(V(2)));

    thdi = sqrt(irms^2 - ilrms^2) / ilrms * 100;
    thdv = sqrt(vrms^2 - vlrms^2) / vlrms * 100;

    x = [p s pf dpf thdi thdv irms ilrms vrms vlrms];

```

REFERENCES

- [1] D. W. Hart, "Circuit simulation as an aid in teaching the principles of power electronics," *IEEE Transactions on Education*, vol. 36, pp. 10–16, 1993.
- [2] I. Chamas, M. A. El Nokali, "Automated PSpice simulation as an effective design tool in teaching power electronics," *IEEE Transactions on Education*, vol. 47, pp. 415–421, 2004.
- [3] J. O. Attia, *Electronics and Circuit Analysis Using MATLAB, 2nd Edition*. CRC Press, 2004.
- [4] A. S. Sedra, K. C. Smith, *Microelectronic Circuits, 4th Edition*. Oxford University Press, 1998.
- [5] N. Mohan, T. M. Undeland, W. P. Robbins, *Power Electronics: Converters, Applications and Design, 3rd Edition*. New York: John Wiley & Sons, 2003.

- [6] B. W. Sherman, K. A. Hamacher, "Power supply design in the undergraduate curriculum," *IEEE Transactions on Education*, vol. 40, pp. 278–282, 1997.
- [7] K. V. Cartwright, "Further results related to power supply design and analysis in the undergraduate curriculum," *IEEE Transactions on Education*, vol. 44, pp. 262–267, 2001.
- [8] J. W. Kolar, *Grundlagen der Leistungselektronik*, lecture notes, ETH Zurich, 2006.